J Mater Sci (2008) 43:4475–4482
DOI 10.1007/s10853-008-2653-7

Retardation of grain growth and cavitation by an electric field during superplastic deformation of ultrafine-grained 3Y-TZP at 1,450–1,600 °C

Di Yang · Hans Conrad

Received: 17 December 2007 / Accepted: 14 April 2008 / Published online: 29 April 2008

Abstract The influence of a continuous dc electric field applied orthogonal to the tensile direction on the flow stress, grain growth, and cavitation during superplastic deformation (SPD) of ultrafine-grained 3Y-TZP at 1,450–1,600 °C was determined. The field gave a significant reduction in the level of the stress-strain curve, and reduced grain growth and cavitation. The decrease in flow stress by the field was attributed mainly to the retardation of grain growth. The decrease in cavitation correlated with the retardation of grain growth and was attributed largely to the reduction in flow stress by the field.

Introduction

It has been determined that significant grain growth [1] and cavitation [2, 3] occur during the superplastic deformation (SPD) of ultrafine-grained, yittria-stabilized tetragonal zirconia polycrystals (Y-TZP). Nieh and Wadsworth [1] reported that the *dynamic* grain growth is given by

$$d^3 = d_o^3 = A \exp -(520 \text{ kJ/mole}/RT)t \quad (1)$$

where d is the grain size at a given time t (or strain), d_o that prior to deformation, and A a constant. They proposed that the magnitude of the grain size exponent $m = 3$ indicated that the grain growth was controlled by solute or impurity drag and that the value of the activation energy $Q = 520$ kJ/mole was close to that for grain boundary diffusion in Y-TZP. Similar values of m and Q have been reported for *static* grain growth in Y-TZP [1, 4–6]. Hwang and Chen [6] interpreted their results on the effect of different solutes on static grain growth in Y-TZP in terms of a drag related to the existing space charge.

Regarding cavitation, it has been reported that the cavities which develop during SPD of Y-TZP originate at triple points [2]. Cavitation was found to increase with decrease in temperature at a fixed strain rate, and initially increase, go through a maximum, and then decrease with increase in strain rate at a given temperature [3]. These behaviors suggested that cavity growth is not solely governed by diffusion, but that stress plays a significant role [1, 3]. A model for cavitation growth which includes both stress and diffusion has been developed by Evans et al. [7].

In prior work by the present authors [8] it was discovered that the application of a dc electric field during the SPD of 3Y-TZP at 1,500 °C reduced both dynamic grain growth and cavitation, and gave an increase in elongation. An electric field thus provides a means for improving the ductility of ceramics. The objective of the present investigation was to obtain further information on the influence of an electric field on dynamic grain growth and cavitation during SPD of Y-TZP.

Experimental

Tensile specimens with a gage section 3.5 × 1.5 × 19 mm were prepared in the manner described in [8]. Briefly, they were prepared by compacting to-shape (70 MPa pressure at room temperature) 3 mole pct. Y-TZP powder purchased from Tosoh Corp. and then sintered in air following the recommended heating schedule shown in Fig. 1. The mean linear intercept grain size of the sintered specimens was 0.40 μm measured on SEM micrographs (Fig. 2) and the

D. Yang · H. Conrad (✉)
Materials Science and Engineering Department, North Carolina State University, Raleigh, NC 27695-7907, USA
e-mail: hans_conrad@ncsu.edu

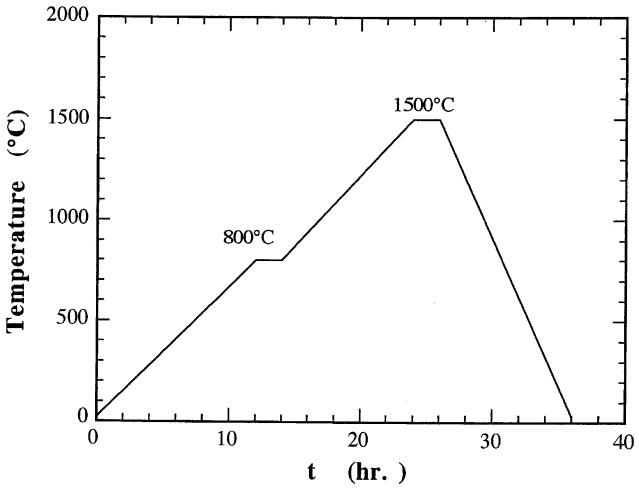

Fig. 1 Temperature versus time schedule employed in sintering the tensile specimens

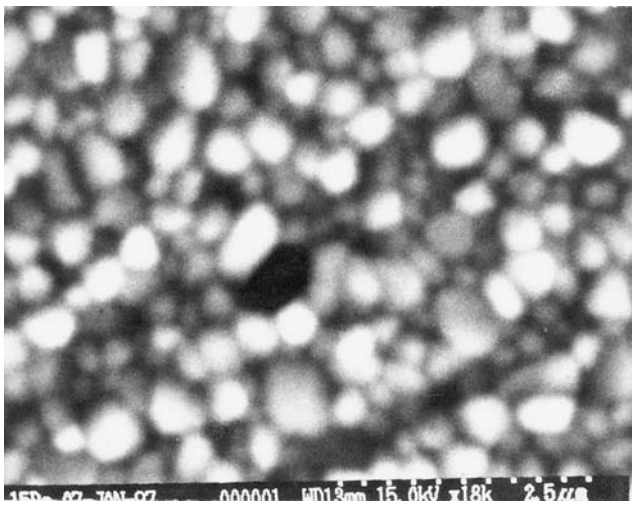

Fig. 2 SEM micrograph of a sintered specimen

volume fraction of porosity determined by precision density measurement was 0.58%. The amount of cubic ZrO_2 was <5%, the sensitivity limit of our x-ray diffraction measurements.

Tensile tests were performed on the sintered specimens at 1,450, 1,500, and 1,600 ± 1 °C without and with a continuous dc electric field at an initial strain rate $\dot{\epsilon}_o = 1.3 \times 10^{-4} s^{-1}$ employing the fixture and electrical

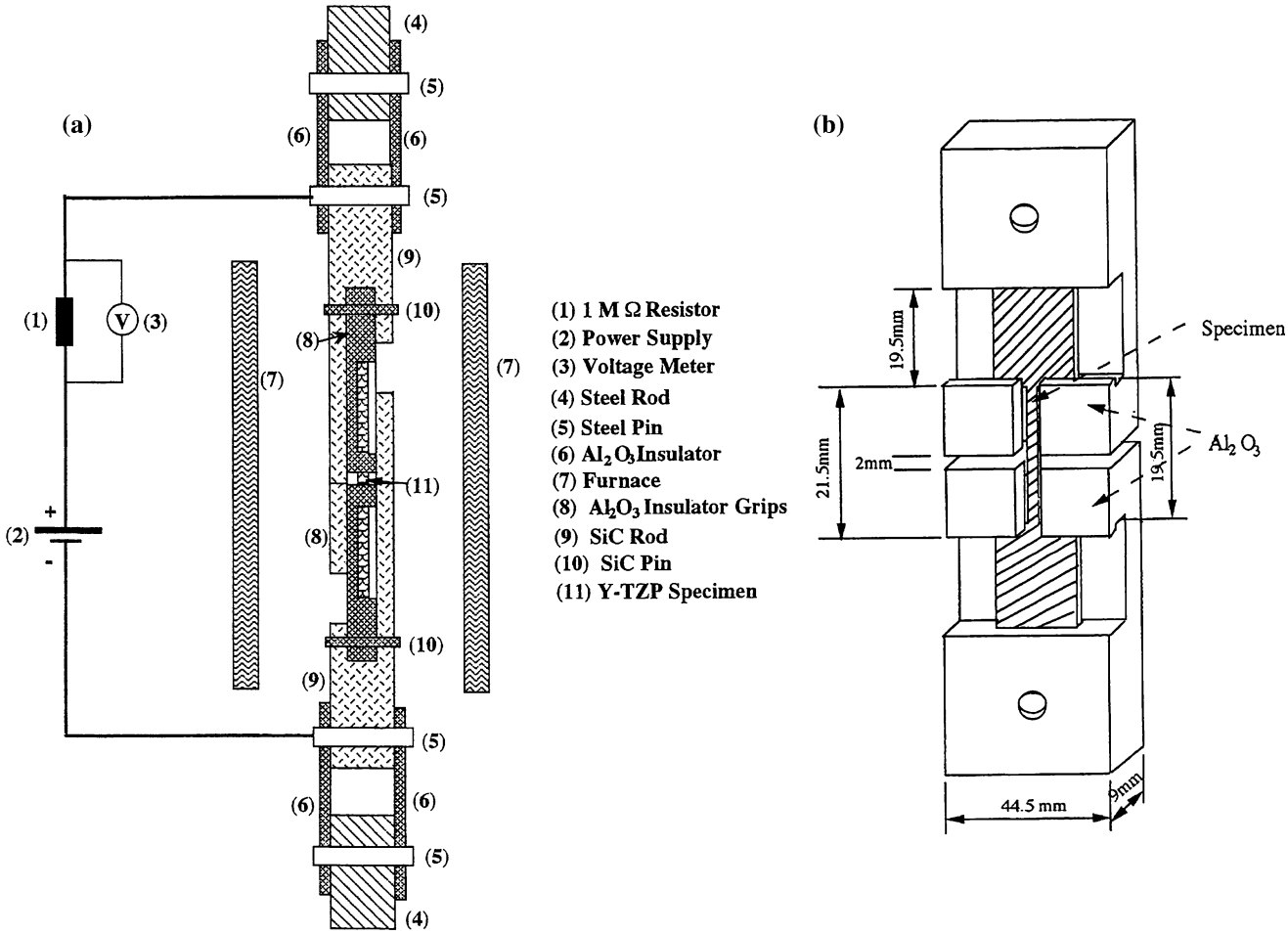

Fig. 3 (**a**) Tensile loading fixture and electrical arrangement. (**b**) Specimen grip fixture

arrangement shown in Fig. 3a. A detailed view of the grip fixture is given in Fig. 3b. The electric field was applied by two planar, parallel (separated by 2 cm), conducting SiC electrodes connected to the dc power supply. The specimen was located midway between the two oppositely charged SiC electrodes, so that an air gap existed between the specimen and each electrode, i.e. there was no direct contact of the specimen with the electrodes. During a tensile test with electric field the power supply voltage was held constant at 2 kV, giving a *nominal* electric field $E_a = 1$ kV/cm between the two SiC electrodes.

In addition to tests without and with electric field at constant strain rate throughout, strain rate change tests in which the crosshead speed was alternately increased and decreased by a factor of ten were performed on a separate set of specimens to give the stress exponent $n = \partial \log \dot{\in} / \partial \log \sigma$ as a function of strain. True stress and true strain in all tension tests were determined from recordings of the load and the machine crosshead displacement.

Following abrasive polishing and thermal etching, SEM micrographs were taken at two locations in both halves of the fractured tensile specimens which had been tested without and with electric field: (a) the grip tab ($\varepsilon \approx 0$) and (b) near the fracture surface where the measured strain from the decrease in cross section area $\varepsilon \approx 1.0$. The mean linear intercept grain size d and the volume fraction of cavities V_c were determined on the SEM micrographs. The value of d was obtained from $\sim$200 counts along random lines drawn on each micrograph; V_c was determined by the point counting technique.

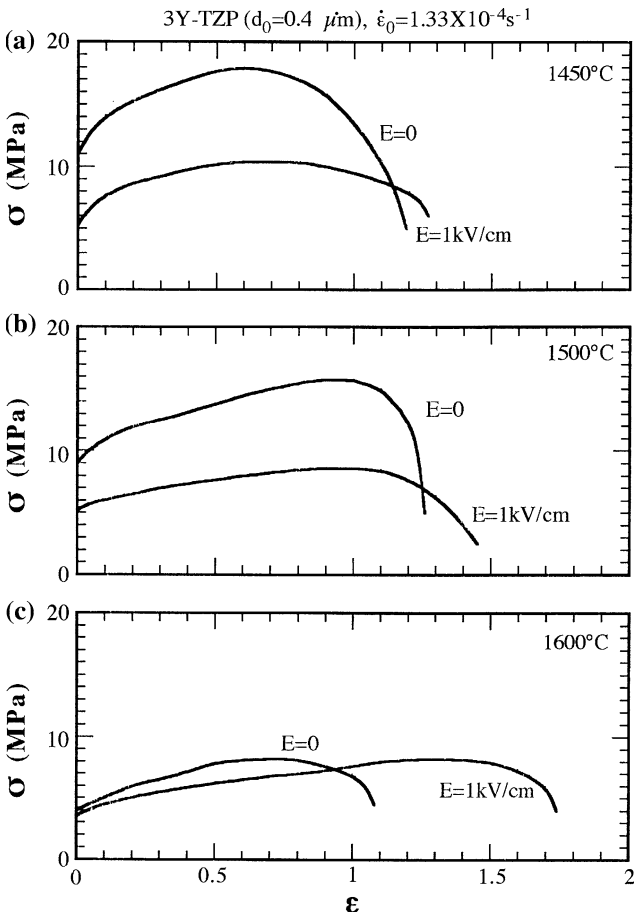

Fig. 4 True stress-strain curves without and with electric field at 1,450, 1,500, and 1,600 °C

Results

Flow stress and elongation

True stress σ versus true stain $\in$ curves for the specimens tested without and with electric field at 1,450–1,600 °C are given in Fig. 4. To be noted is that the curves with field all lie below those without field, the difference between the two increasing with decrease in temperature. Also to be noted is that the field gave an increase in the fracture strain, $\in_F = \ln(\ell_F/\ell_o)$, the magnitude of which increased with temperature. The increase in ductility produced by the field is further shown in Fig. 5, where the total elongation $e_t = \Delta\ell_F/\ell_o$ is plotted versus temperature.

An example of the behavior in the strain rate change tests is given in Fig. 6. The values of $n = \log(\dot{\in}_2/\dot{\in}_1)/\log(\sigma_2/\sigma_1)$ versus strain for the tests without and with field at 1,450–1,600 °C are presented in Fig. 7. To be noted is that n is essentially independent of electric field over the entire strain and temperature ranges. There exists however a tendency for n to decrease with strain and also slightly

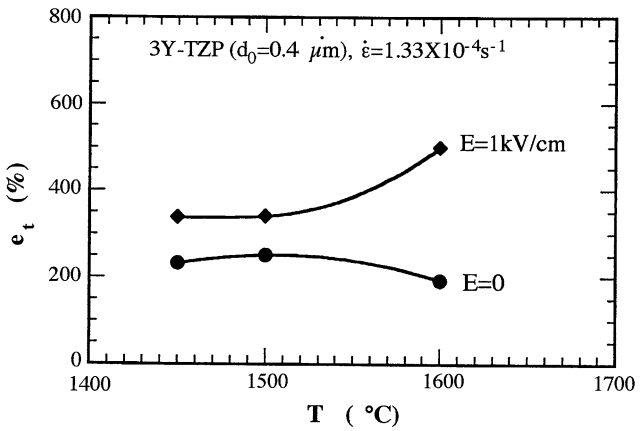

Fig. 5 Total elongation without and with electric field at 1,450, 1,500, and 1,600 °C

with temperature. The present values of n are in accord with those reported by Jiménez-Melando et al. [9] for the plastic deformation kinetics of Y-TZP at high temperatures.

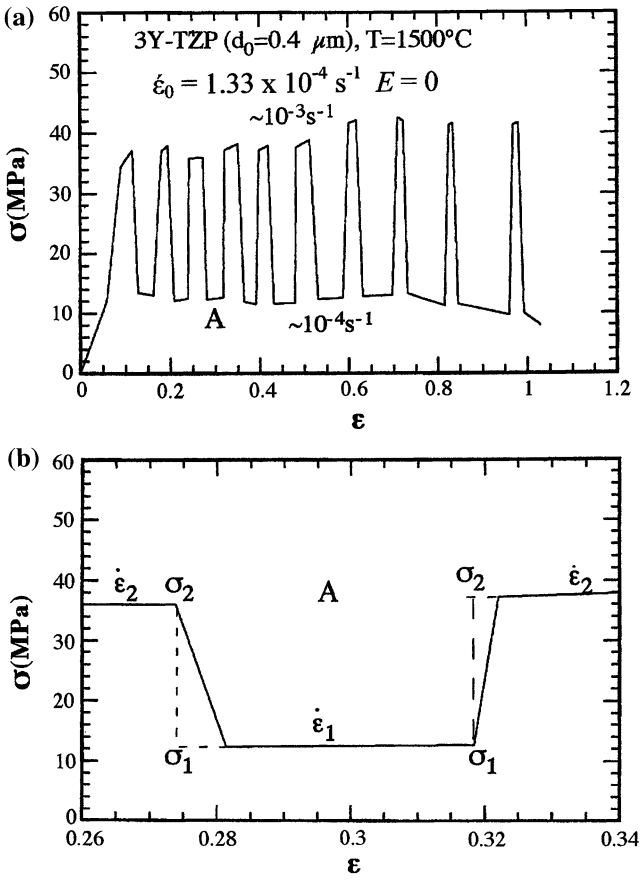

Fig. 6 (**a**) Strain rate change tests at 1,500 °C with $E = 0$. (**b**) Behavior at location A

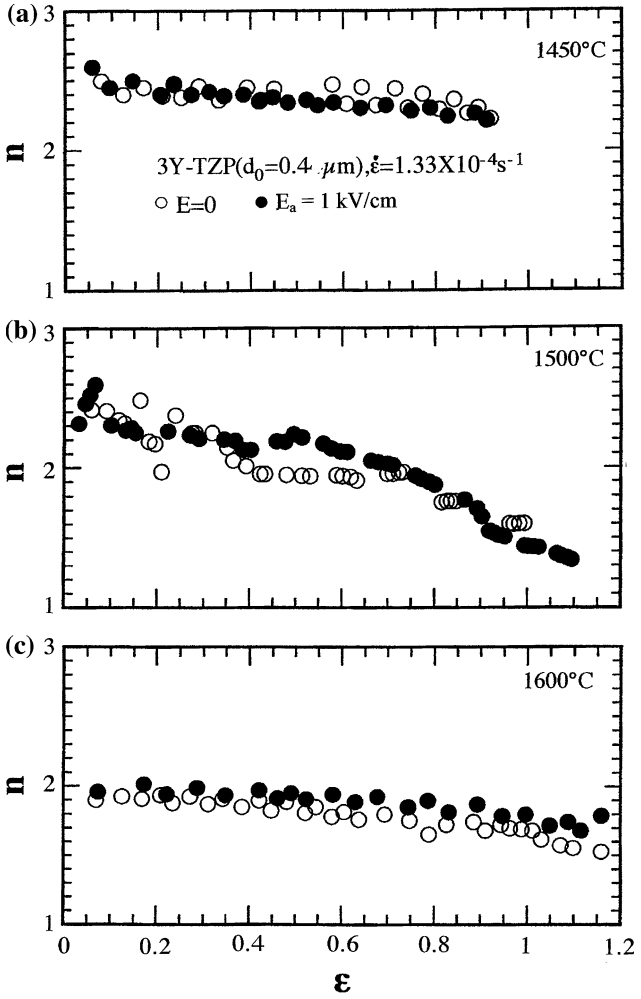

Fig. 7 The stress exponent $n = \log(\dot{\epsilon}_2/\dot{\epsilon}_1)/\log(\sigma_2/\sigma_1)$ versus strain for the tests at 1,450–1,600 °C without and with electric field

Grain growth and cavitation

The microstructure in the vicinity of the fracture of the specimen tested with electric field at 1,600 °C is shown in Fig. 8. Positions (a) and (b) are at the edge of the specimen adjacent to the fracture, while position (c) is further back from the fracture. To be noted is that appreciable cavitation occurred at positions (a) and (b), with considerably less at (c), and to the right of this position. Hence, all measurements of grain size and cavitation at $\epsilon \approx 1.0$ were made at a location to the right of position (c). As examples, SEM micrographs at the grip region ($\epsilon \approx 0$) and near the fracture surface ($\epsilon \approx 1.0$) for the tests at 1,500 °C without and with electric field are presented in Figs. 9 and 10, respectively. To be noted is that at each of the two locations the electric field retarded both grain growth and cavitation. The average values of d and V_c from all micrographs, and the scatter in values between micrographs, are given in Table 1. Figures 11 and 12, are plots of the average values of d and V_c versus temperature, respectively, for tests without and with electric field. In Fig. 11 both the static ($\epsilon \approx 0$) and dynamic ($\epsilon \approx 1.0$) grain size increased with temperature, the retarding effect of the field being greater for dynamic grain growth compared to static growth. In Fig. 12 it is seen that the average cavitation V_c goes through a maximum at ~1,500 °C for both strain levels, the retarding effect of the field being greatest at this temperature. Again, the retarding effect is larger at the higher strain level.

Discussion

Grain growth

Theoretical considerations [10, 11] for the rate of grain growth give

$$\dot{d} = (PM)^m \tag{2}$$

where P is the driving force and $M = M_o \exp(-Q_d/RT)$ the grain boundary mobility, $m = 1$ for pure materials but may be greater than one with the presence of impurities or solutes. The results by Nieh and Wadswroth (NW) [1]

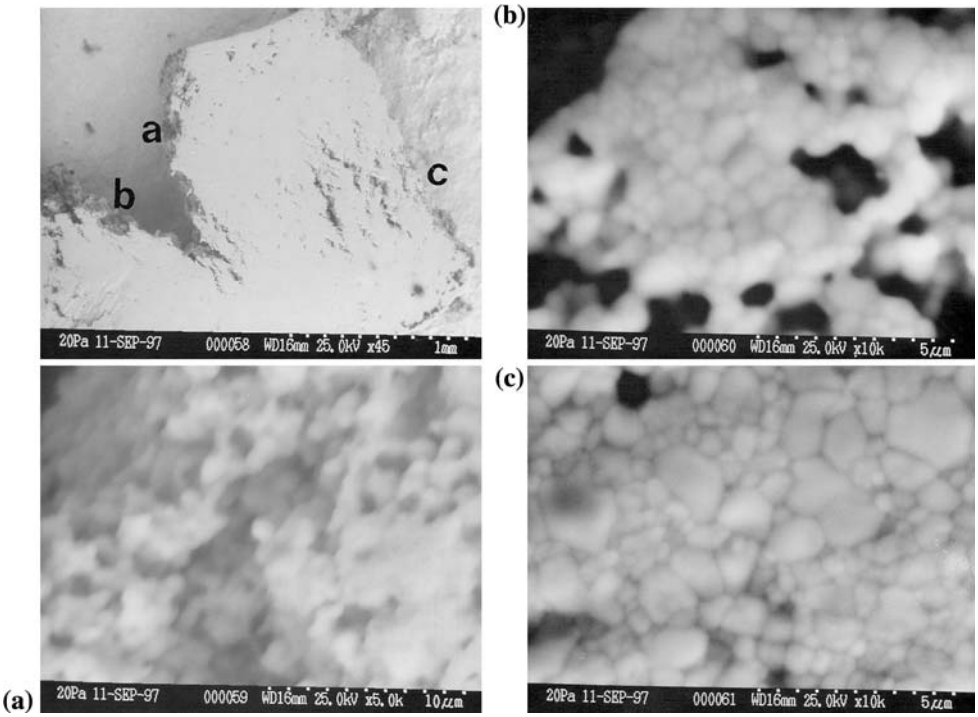

Fig. 8 SEM micrographs taken near the fracture surface of a specimen tested at 1,600 °C with electric field. (**a**), (**b**), and (**c**) are enlarged views of the corresponding positions in the fracture region

(Eq. 1) give $m = 2$ and Q_d = 520 kJ/mole, which suggests that grain growth in Y-TZP is governed by either impurities or the yittria solute atoms. Since in the present tests some grain growth could occur during heating to the test temperature, the magnitude of d_o is not known. Hence, a direct comparison of the present results without field and those by NW is not feasible. However, the magnitudes of the present grain sizes and their temperature dependence are similar to those in [1].

According to Eq. 2 the retarding effect of the electric field on grain growth could be due to either, or both, a reduction in the product M_oP or an increase in the activation energy Q_d. If the dominant effect of the applied field E_a were to increase Q_d, one expects that the ratio of the grain size with field divided by that without field (d_E/d) would increase with test temperature, otherwise the dominant effect would be on the product PM_o. The results obtained in the present tests (Fig. 11) do not provide a clear resolution of this question. However, in case of polycrystalline NaCl it was discovered [12] that the retarding effect of the field on both static and dynamic grain growth was through its reduction of the pre-exponential. Since an important parameter regarding the driving force P is the grain boundary energy γ_{gb}, i.e. $P = 2\gamma_{gb}/d$ [11], one possibility is that the field reduces γ_{gb}, thereby giving a decrease in grain growth rate.

Cavitation

The reason for the larger V_c in the grip region ($V_c \approx$ 1–3 %), where supposedly $\in \approx 0$, compared to the as-sintered value (0.54% - 0.58%) is not clear. It could be due to one or more of the following: (a) emission of residual dissolved or occluded gases (b) thermal-expansion anisotropy of the grains, and (c) some plastic deformation in the grip region. The slightly larger effect of E_a on V_c for $\in \approx 0$ at 1,500 °C in Fig. 12 is within experimental scatter and may not be real. The more pronounced anomalous temperature dependence of V_c for $\in = 1.0$ is however similar to the anomalous effect of strain rate on cavitation in Y-TZP reported by Schissler et al. [2]. These anomalies suggest that both diffusion and stress play a role in cavitation, or that a different mechanism governs cavitation between 1,400° and 1,500° compared to higher temperatures. Regarding the latter, Dillon and Harmer [13] have identified different types of grain boundary structures in alumina which have different grain boundary motility mechanisms.

Of further interest are the mechanism(s) responsible for the reduction in cavitation by the electric field. Figure 13 shows that the ratio of the volume fraction of the cavities with field ($V_{c,E}$) to that without field (V_c) increases with the ratio of the corresponding grain sizes. This suggests that the decrease in cavitation by the field is related to the decrease in grain size. A reduction in grain size gives two conditions which would reduce cavitation: (a) a reduction in the flow stress and (b) a decrease in the grain boundary sliding distance. Both reduce the stress concentration at triple points. The fact that the effect of E_a on d is relatively independent of temperatures (Fig. 11), while the effect of E_a on V_c is maximum at 1,500 °C (Fig. 12) indicates that influence of temperature on the mechanism governing

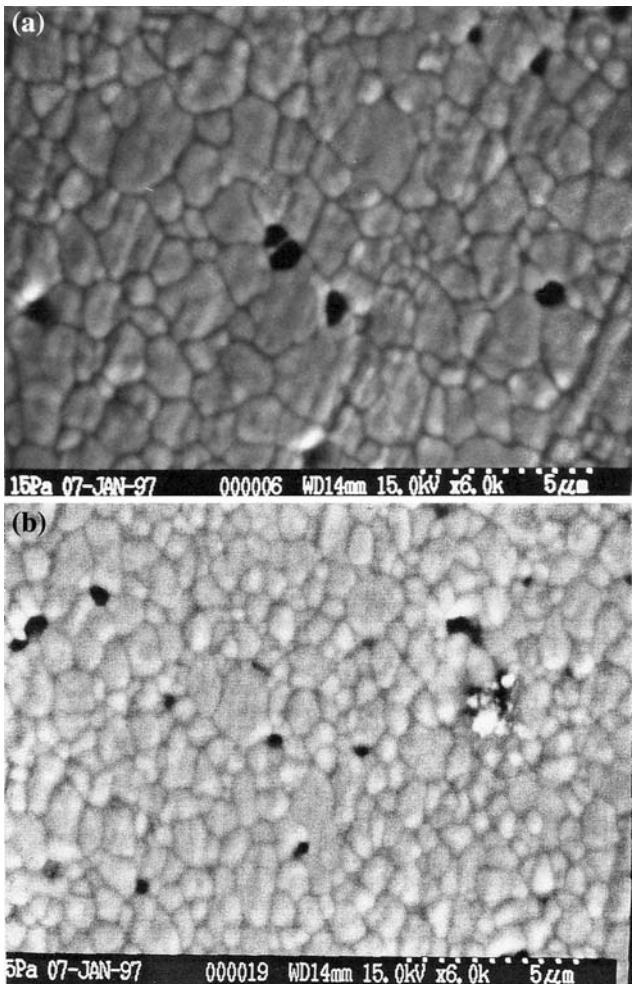

Fig. 9 SEM micrographs of the grip region ($\in \approx 0$) of the specimens fractured at 1,500 °C: (**a**) $E = 0$ and (**b**) E_a = 1 kV/cm

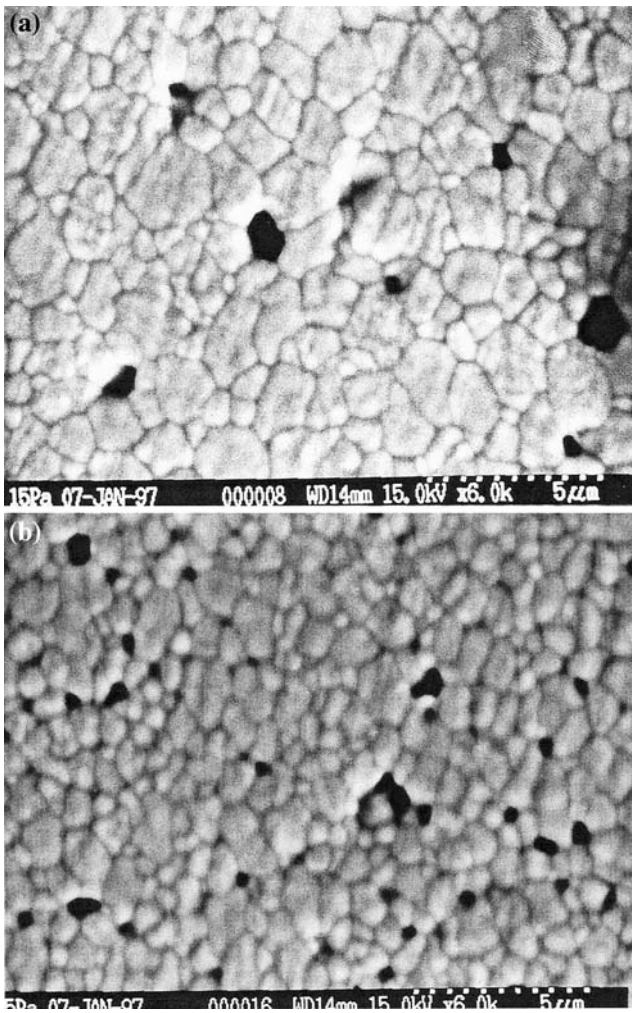

Fig. 10 SEM micrographs near the fracture surface ($\in \approx 1.0$) of the specimens deformed at 1,500 °C: (**a**) $E = 0$ and (**b**) E_a = 1 kV/cm

grain growth differs from that governing cavitation. This is in accord with theoretical considerations of grain growth [10, 11] and of cavitation [7, 14], which give different temperature dependencies for these respective phenomena. Our understanding of the effect of E_a on the physical mechanisms governing them is however still unclear.

Mechanical properties

Based on the detailed review of the literature on the plastic deformation kinetics of ultrafine-grained Y-TZP at high temperatures by Jiménez-Melando et al. [9] and considering the model by Ashby and Verrel [15], the following constitutive equation was proposed [16, 17]

$$\dot{\in} = \frac{A}{T}\left(\frac{b}{d^2}\right)\left(\frac{\sigma - \sigma_o}{\mu}\right)\Omega D_\ell^{Zr^{4+}} \tag{3}$$

where $\dot{\in}$ is the strain rate, A a constant, T the temperature, b the Burgers vector, d the grain size, σ the applied stress, σ_o a threshold stress, μ the elastic modulus, Ω the atomic volume, and $D_\ell^{Zr^{4+}}$ the lattice diffusion of the Zr^{4+} ions. Furthermore, it was determined [16, 17] that the decrease in flow stress $\Delta\sigma_E = \sigma - \sigma_E$ which resulted from application of an electric field consisted of three components, i.e.,

$$\Delta\sigma_E = \Delta\sigma_T + \Delta\sigma_E^{*,b} + \Delta\sigma_E^{str} \tag{4}$$

where $\Delta\sigma_T$ is the decrease due to Joule heating, $\Delta\sigma_E^{*,b}$ that due to the direct effect of the field on the plastic deformation kinetics, and $\Delta\sigma_E^{str}$ that due to the effect of the field on the microstructure, i.e. on the grain size. According to Eq. 3, the flow stress σ_E^d at constant T and $\dot{\in}$ which corresponds to the measured grain size with electric field d_E is given by

$$\sigma_E^d = \sigma(d_E/d)^2 \tag{5}$$

and in turn when $\Delta\sigma_T$ and $\Delta\sigma_E^{*,b}$ are small and $\sigma_0 = \sigma\,(n-1)/n$ [16, 17] one obtains

Table 1 Effect of electric field E_a on the mean liner intercept grain size d and the volume fraction of cavities V_c at $\varepsilon \approx 0$ (grip) and at $\varepsilon \approx 1.0$ (near fracture)

T °C	ε	E_a (kV/cm)	*No.*[a]	d^b_{min} (μm)	d^c_{avg} (μm)	d^d_{max} (μm)	$V^b_{c,max}$ (%)	$V^c_{c,avg}$ (%)	$V^d_{c,max}$ (%)
1,450	0	0	4	0.69	0.74	0.84	1.07	1.15	1.22
	0	1	4	0.70	0.77	0.94	1.10	1.13	1.22
	1	0	5	0.69	0.98	1.43	1.33	2.20	4.74
	1	1	2	0.69	0.71	0.73	0.80	1.40	1.99
1,500	0	0	6	1.01	1.08	1.21	0.80	2.72	3.20
	0	1	4	0.64	0.85	0.87	1.14	2.15	4.40
	1	0	4	1.09	1.11	1.13	2.70	6.78	9.60
	1	1	5	0.59	0.61	0.63	1.20	3.77	7.20
1,600	0	0	2	1.14	1.18	1.21	1.22	1.56	1.89
	0	1	3	0.94	1.14	1.24	1.22	1.77	2.68
	1	0	2	1.32	1.38	1.43	1.54	1.75	1.96
	1	1	2	0.81	1.03	1.25	1.07	1.59	2.10

[a] Number of SEM micrographs taken at the specified location

[b] d_{min} and $V_{c,min}$ refer to the respective micrographs with the smallest mean linear intercept grain size or volume fraction of cavitation at a given location

[c] d_{avg} and $V_{c,avg}$ refer to the average values from all micrographs at a given location

[d] d_{max} and $V_{c,max}$ refer to the respective micrographs with the largest values at a given location

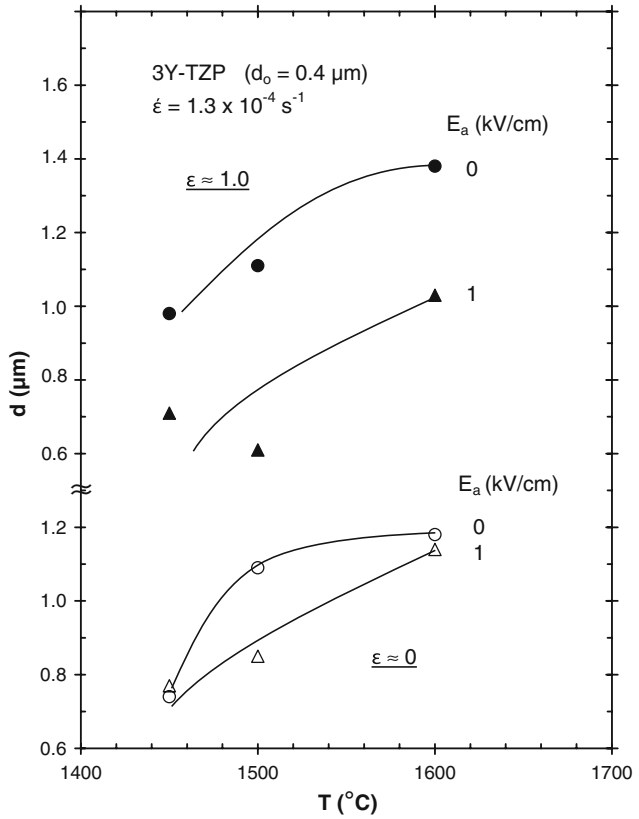

Fig. 11 Effect of electric field on grain size in the grip region ($\in \approx 0$) and near the fracture surface ($\in \approx 1.0$) for the tests at 1,450–1,600 °C

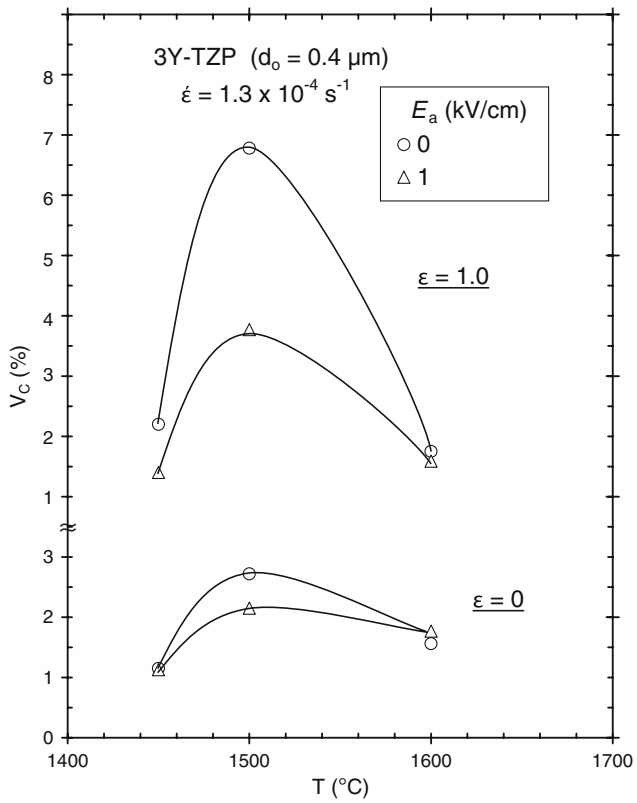

Fig. 12 Effect of electric field on the volume fraction of cavitation in the grip region ($\in \approx 0$) and near the fracture surface ($\in \approx 1.0$) for the tests at 1,450–1,600 °C

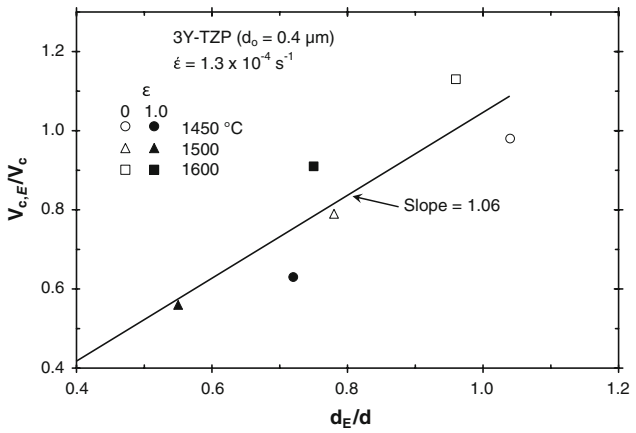

Fig. 13 Cavitation ratio for tests with and without electric field versus corresponding grain size ratio

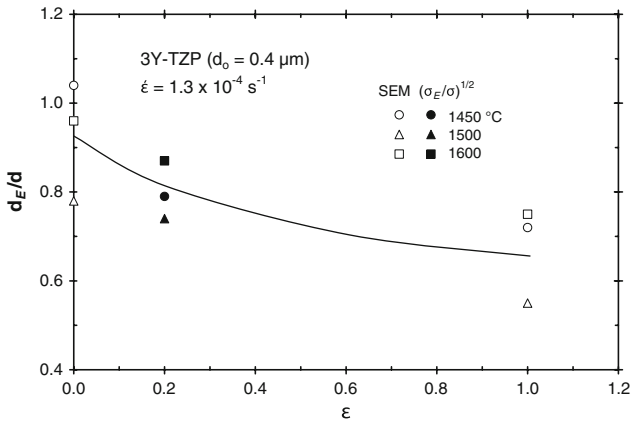

Fig. 14 Grain size ratio d_E/d with and without electric field versus strain determined from SEM measurements and calculated from the flow stress

$$d_E/d \approx (\sigma_E/\sigma)^{1/2} \tag{5a}$$

where σ and d are the flow stress and grain size, respectively, without field. In Fig. 14 the values of d_E/d at $\epsilon = 0.2$ calculated employing Eq. 5a are compared with the values of d_E/d determined from the SEM measurements at $\epsilon = 0$ and $\epsilon = 1.0$ (Fig. 11). In keeping with the previous work [16, 17] the values of σ and σ_E were chosen at $\epsilon = 0.2$ to reduce any effects of grip alignment at smaller strains and cavitation at larger strains. It is seen in Fig. 14 that the values of d_E/d calculated employing Eq. 5a are in reasonable accord with the SEM measurements. This indicates that the major influence of the electric field on the flow stress in the present tests is through its retardation of grain growth.

Summary and conclusions

The influence of a continuous dc electric field applied orthogonal to the tensile direction on the flow stress, grain growth and cavitation in ultrafine-grained 3Y-TZP was determined at 1,450–1,600 °C. The field was applied by placing the specimen midway between two oppositely charged SiC electrodes separated by an air gap of 2 cm to give a nominal electric field E_a = 1 kV/cm between the electrodes. The field gave a significant reduction in the level of the stress-strain curve and retarded grain growth and cavitation measured on SEM micrographs. A major portion of the reduction in flow stress could be attributed to the observed retardation of grain growth. Cavitation led to an ultimate decreased in the flow stress and fracture.

The retardation of grain growth by the field appears to be mainly through a reduction of the pre-exponential term in the grain growth equation due to a decrease in the grain boundary energy. The retardation of cavitation correlated with the retardation of grain growth and was attributed in large part to the reduction in flow stress by the field.

Acknowledgements This research was supported by the US Army Research Laboratory and the US Army Research Office under Grant Nos. DAAH04-94G-0311 and DAA19-02-1-0315 with Drs. W. Simmons and W. Mullins, respectively, as contract monitors. The authors wish to thank Rachel Wolfe for typing the manuscript and Stephen Starnes for preparing the illustrations.

References

1. Nieh T-G, Wadsworth J (1989) J Am Ceram Soc 72:1469. doi:10.1111/j.1151-2916.1989.tb07678.x
2. Schissler DJ, Chokshi AH, Nieh T-G, Wadsowrth (1991) J Acta Metall Mater 39:3227. doi:10.1016/0956-7151(91)90057-8
3. Zhou M, Ma Y, Langdon TG (1995) In: Bradt RC et al (eds) Plastic deformation of ceramics. Plenum Press, New York, p 301
4. Stato T, Nauer M, Carry C (1991) J Am Ceram Soc 74:2615. doi:10.1111/j.1151-2916.1991.tb06809.x
5. Nauer N, Carry C (1992) Materials Science Forum, Trans Tech Publications, Switzerland 94–96:871
6. Hwang S-L, Chen I-W (1991) J Am Ceram Soc 73:3268
7. Evans AG, Rice JR, Hirth JP (1980) J Am Ceram Soc 63:368. doi:10.1111/j.1151-2916.1980.tb10194.x
8. Yang Di, Conrad H (1997) Scripta Mater 36:1431. doi:10.1016/S1359-6462(97)00045-6
9. Jiménez-Melando M, Dominguez-Rodriguez A, Bravo-Leon A (1998) J Am Ceram Soc 81:2761
10. Cahn JW (1962) Acta Metall 10:789. doi:10.1016/0001-6160(62)90092-5
11. Lücke K, Stüwe HP (1963) In: Himmel Z (ed) Recovery and recrystallization of metals. Gordon and Breach, New York, p 171
12. Yang Di, Conrad H (1998) Scripta Mater 38:1443. doi:10.1016/S1359-6462(98)00042-6
13. Dillon SJ, Harmer MP (2007) Acta Mater 55:5247. doi:10.1016/j.actamat.2007.04.051
14. Tanaka T, Takigawa Y, Higashi K (2008) Scripta Mater 58:643. doi:10.1016/j.scriptamat.2007.11.028
15. Ashby MF, Verrall RA (1973) Acta Metall 21:149. doi:10.1016/0001-6160(73)90057-6
16. Conrad H, Yang Di, Becher P (2008) Mater Sci Eng A 477:358. doi:10.1016/j.msea.2007.05.057
17. Conrad H, Yang Di (2007) Acta Mater 55:6789. doi:10.1016/j.actamat.2007.08.032